Controlling the Coordination Mode of 1,4,7-Triazacyclononane Complexes of Rhodium and Iridium and Evaluating Their Behavior as Phenylacetylene Polymerization Catalysts

Andrew L. Gott, Patrick C. McGowan,* and Claire N. Temple

School of Chemistry, University of Leeds, Woodhouse Lane, Leeds LS2 9JT, U.K.

Received February 26, 2008

A number of κ^1- and κ^3-triazacyclononane Rh^I, Ir^1, Rh^{III}, and Ir^{III} derivatives have been synthesized and characterized, with conversion from κ^1-triazacyclononane complexes to κ^3-derivatives. The results of the catalytic studies show that the Rh(I) and Ir(I) complexes polymerize phenylacetylene more effectively than $[M(COD)(\mu\text{-Cl})]_2$ (M = Rh and Ir).

Introduction

We have been interested in late metal complexes of 1,4,7-triazacyclononane[1,2] as an alternative[3] to cyclopentadienyl for some time due to the different steric and electronic properties conferred upon the metal. Numerous reports of 1,4,7-triazacyclononane complexes of Rh exist in the literature;[4–7] in comparison, the chemistry of Ir derivatives is less well developed[8] due to unwanted reduction processes,[9] and the applications of Rh/Ir complexes in catalytic systems are relatively sparse.[6,10] In this contribution we describe the facile synthesis of novel Rh and Ir complexes of 1,4,7-triazacyclononane, a study of the coordination mode of the di-N-substituted macrocyclic ring, including a detailed structural study of the products. The activity of the described complexes in the polymerization of phenylacetylene is reported.

In the literature there are many examples of early transition-metal catalysts that are capable of polymerizing such alkynes to yield polyenes, in particular sterically hindered alkynes. Polyenes are polymers that contain conjugated backbones and are highly desirable materials owing to their unique physicochemical properties. These include conductivity, oxygen permeability, unique ferromagnetic, photolithographic, and optoelectronic properties, and liquid crystallinity, with possible uses in low-weight/high-charge batteries, polymer modified electrodes, capacitors, nonlinear optics, and humidity sensors.[11,12] Polyacetylene itself is sensitive to oxygen, insoluble, and difficult to process. Substituents present in the monomers are needed to improve these qualities for industrial application. One alternative is phenylacetylene, as polyphenylacetylene is stable in air, soluble, and easier to process.

Known catalysts capable of mediating the polymerization of phenylacetylene include compounds of molybdenum, tungsten, niobium, and tantalum,[11] which generally need a cocatalyst; their main disadvantage is that the complexes are highly oxophilic, and therefore they cannot tolerate certain functional groups on substituted monomers. This necessitates that polymerizations must be carried out in strictly oxygen- and moisture-free conditions; in contrast late metal complexes such as Rh and Ir are tolerant of air and water. Consequently, a number of Rh(I) and Ir(I) complexes have been reported as catalysts for the production of polyphenylacetylene,[13,14] and it is to this end we report a new catalytic system. Part of this work has been reported previously and is discussed here with respect to the catalytic activity.[2]

Results and Discussion

M(III) Complex Synthesis. The complexes **1**[2] and **2** were prepared as shown in Scheme 1, via reaction between 1,4-diisopropyl-1,4,7-triazacyclononane and $[Cp^*MCl(\mu\text{-Cl})]_2$ (M = Rh, Ir) in THF and methylene chloride, respectively, to yield air-stable compounds. X-ray crystallographic analyses of complexes **1**[2] and **2** showed that the macrocyclic ring was bound to the metal center through one nitrogen only. This was surprising since few other examples exist; two tantalum(V) compounds, reported elsewhere by Arnold and co-workers,[15] are the only

* To whom correspondence should be addressed. E-mail: p.c.mcgowan@leeds.ac.uk. Tel: (+44) 0113 343 6404. Fax: (+44) 0113 343 6565.

(1) (a) Gott, A. L.; McGowan, P. C.; Podesta, T. J.; Tate, C. W. *Inorg. Chim. Acta* **2004**, *357*, 689. (b) Gott, A. L.; McGowan, P. C.; Podesta, T. J.; Thornton-Pett, M. *J. Chem. Soc., Dalton Trans.* **2002**, 3619. (c) McGowan, P. C.; Podesta, T. J.; Thornton-Pett, M. *Inorg. Chem.* **2001**, *40*, 1445.

(2) Gott, A. L.; McGowan, P. C.; Temple, C. N. *Dalton Trans.* **2004**, 1841.

(3) Cui, C. M.; Giesbrecht, G. R.; Schmidt, J. A. R.; Arnold, J. *Chem. Commun.* **2003**, 1025.

(4) (a) Hanke, D.; Wieghardt, K.; Nuber, B.; Lu, R. S.; McMullan, R. K.; Koetzle, T. F.; Bau, R. *Inorg. Chem.* **1993**, *32*, 4300. (b) Wieghardt, K.; Chaudhuri, P.; Nuber, B.; Weiss, J. *Inorg. Chem.* **1982**, *21*, 3086. (c) Wieghardt, K.; Schmidt, W.; Nuber, B.; Prikner, B.; Weiss, J. *Chem. Ber.* **1980**, *113*, 36.

(5) (a) Flood, T. C.; Janak, K. E.; Iimura, H.; Zhen, H. *J. Am. Chem. Soc.* **2000**, *122*, 6783. (b) Zhen, H.; Wang, C.; Hu, Y.; Flood, T. C. *Organometallics* **1998**, *17*, 5397. (c) Zhou, R. J.; Wang, C. M.; Hu, Y. H.; Flood, T. C. *Organometallics* **1997**, *16*, 434. (d) Wang, L.; Wang, C. M.; Bau, R.; Flood, T. C. *Organometallics* **1996**, *15*, 491. (e) Wang, C.; Ziller, J.; Flood, T. *J. Am. Chem. Soc.* **1995**, *117*, 1647.

(6) Wang, L.; Flood, T. C. *J. Am. Chem. Soc.* **1992**, *114*, 3169.

(7) (a) de Bruin, B.; Brands, J. A.; Donners, J. J. J. M.; Donners, M. P. J.; de Gelder, R.; Smits, J. M. M.; Gal, A. W.; Spek, A. L. *Chem.−Eur. J.* **1999**, *5*, 2921. (b) de Bruin, B.; Donners, J. J. J. M.; de Gelder, R.; Smits, J. M. M.; Gal, A. W. *Eur. J. Inorg. Chem.* **1998**, 401. (c) Baker, M. V.; Brown, D. H.; Skelton, B. W.; White, A. H. *J. Chem. Soc., Dalton Trans.* **2002**, *2595*, 7. (d) Hayashi, H.; Nishida, H.; Ogo, S.; Fukuzumi, S. *Inorg. Chim. Acta* **2004**, *357*, 2939.

(8) (a) Flood, T. C.; Iimura, H.; Perotti, J. M.; Rheingold, A. L.; Concolino, T. E. *Chem. Commun.* **2000**, 1681. (b) Gajhede, M.; Simonsen, K.; Skov, L. K. *Acta Chem. Scand.* **1993**, *47*, 271.

(9) Flensburg, C.; Simonsen, K.; Skov, L. K. *Acta Chem. Scand.* **1994**, *48*, 209.

(10) (a) Wang, L.; Lu, R. S.; Bau, R.; Flood, T. C. *J. Am. Chem. Soc.* **1993**, *115*, 6999. (b) Sari, T.; Tuula, P.; Tapani, P.; Ove, A.; Hilkka, K. *Int. Pat. Appl. WO9616958*, 1996.

(11) Claverie, J. P.; Soula, R. *Prog. Polym. Sci.* **2003**, *28*, 619.

10.1021/om800180a CCC: $40.75
Publication on Web 05/21/2008

Scheme 1. Synthesis of Rh(III) and Ir(III) Complexes

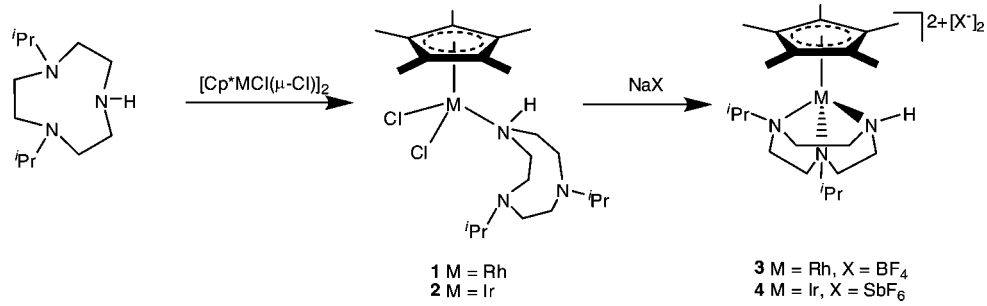

1 M = Rh
2 M = Ir

3 M = Rh, X = BF_4
4 M = Ir, X = SbF_6

Table 1. Data Collection and Refinement Parameters for 2 and 6−11

	2	6	7	8	9	10	11
formula	$C_{44}H_{84}Cl_4Ir_2N_6$	$C_{21}H_{41}Cl_3IrN_3$	$C_{21}H_{39}F_3N_3O_3RhS$	$C_{60}H_{117}F_{18}N_9Rh_3Sb_3$	$C_{20}H_{39}F_6IrN_3Sb$	$C_{28}H_{51}Cl_2N_3Rh$	$C_{28}H_{51}Cl_2N_3Ir$
fw	1223.37	634.12	573.52	1980.61	749.49	706.44	885.02
size (mm)	0.43 × 0.20 × 0.13	0.73 × 0.30 × 0.23	0.40 × 0.26 × 0.17	0.40 × 0.20 × 0.19	0.53 × 0.36 × 0.13	0.30 × 0.10 × 0.10	0.53 × 0.26 × 0.23
morphology	orange block	yellow block	yellow block	yellow block	yellow block	yellow block	yellow block
temp (K)	173(2)	173(2)	173(2)	173(2)	173(2)	173(2)	173(2)
wavelength (Å)	0.71073	0.71073	0.71073	0.71073	0.71073	0.71073	0.71073
cryst syst	orthorhombic	triclinic	monoclinic	monoclinic	monoclinic	monoclinic	monoclinic
space group	*Pbca*	$P\bar{1}$	$P2_1/c$	$P2_1/c$	$P2_1/c$	$P2_1/c$	$P2_1/n$
a (Å)	13.53900(1)	9.46500(10)	9.533(2)	21.590(4)	9.53200(10)	8.57500(10)	8.5172(7)
b (Å)	23.09800(1)	10.88600(10)	10.886(2)	23.061(5)	10.83300(10)	19.6800(10)	19.806(2)
c (Å)	32.27990(2)	14.28600(2)	23.252(5)	14.538(3)	23.0820(4)	19.2590(4)	17.3502(18)
α (deg)	90	70.5890(10)	90	90	90	90	90
β (deg)	90	81.3010(10)	91.0840(10)	98.05(3)	91.3040(10).	115.4810(10)	90.554(6)
γ (deg)	90	65.2690(10)	90	90	90	90	90
V (Å^3)	10094.41(11)	1260.84(2)	2411.81(8)	7167(2)	2382.83(5)	2939.41(8)	2926.7(5)
Z	8	2	4	4	4	4	4
d_{calc} (mg/m^3)	1.61	1.67	1.579	1.836	2.089	1.596	2.009
F(000)	9792	632	1192	3960	1448	1456	1712
no. of reflns collect.	192 275	25 137	28 333	99 439	20 030	40 211	46 708
no. of unique reflns	11 570	5775	5509	16 402	5438	6689	6692
R(int)	0.1944	0.168	0.1237	0.1205	0.2154	0.0967	0.1225
no. of data/restr/params	11 570/17/523	5775/1/262	5509/0/293	16 402/0/886	5438/0/284	6689/0/320	6692/0/320
GOF	1.08	1.061	1.046	1.044	1.061	1.203	1.115
R_1 ($I > 2\sigma I$)	0.0480	0.0569	0.0454	0.0652	0.0548	0.0532	0.0375
wR_2	0.1251	0.1435	0.1148	0.2129	0.1414	0.1368	0.0994

comparable instances. In these cases, the complexes were ultimately formed by salt metathesis and the Ta−N connectivity is formally a metal amido bond rather than dative. The Ta centers are not electronically saturated, and so the steric bulk of the ligand is thought to dictate the binding mode. A similar result is seen here; the least sterically hindered nitrogen atom is coordinated to the metal. The molecular structure of **2** can be seen in Figure 1. Data collection and processing parameters can be found for all of the crystal structures in Table 1, and relevant bond lengths and angles in Table 2. The approximate plane of symmetry seen in the X-ray crystal structure running through the Ir−Cp* centroid and the donor NH of **2** is also observed in the NMR spectra, as only three resonances are observed for the macrocyclic ring carbon atoms.

Halide abstraction by treatment with $NaBF_4$ and $AgSbF_6$ furnished the complexes **3** and **4**, respectively, in an attempt to create vacant coordination sites for the remaining donor groups of the macrocyclic ligand. Single crystals of **3** were grown by the slow diffusion of petroleum ether into a methylene chloride solution at room temperature. The complex crystallized in the space group *Pcmn*, and there are one-and-a-half molecules in the asymmetric unit. The structure of the compound cannot be solved fully due to severe disorder problems within the counterions, cocrystallized solvent molecules, and Cp* moiety, and therefore a detailed discussion of metric parameters is not appropriate; nevertheless

(12) (a) Margio, M.; Marsich, N.; Farnetti, E. *J. Mol. Catal. A: Chem.* **2002**, 187. (b) Li, K.; Wei, G.; Darkwa, J.; Pollak, S. K. *Macromolecules* **2002**, *35*, 4573. (c) Tang, B. Z.; Poon, W. H.; Leung, S. M.; Leung, W. H.; Peng, H. *Macromolecules* **1997**, *30*, 2209.

(13) Saeed, I.; Shiotsuki, M.; Masuda, T. *Macromolecules* **2006**, *39*, 8977.

(14) (a) Filipuzzi, S.; Farnetti, E. *J. Mol. Catal. A: Chem.* **2005**, *238*, 111. (b) Marigo, M.; Millos, D.; Marsich, N.; Farnetti, E. *J. Mol. Catal., A: Chem.* **2003**, *206*, 319. (c) Balcar, H.; Cejka, J.; Sedlacek, J.; Svoboda, J.; Zednik, J.; Bastl, Z.; Bosacek, V.; Vohlidal, J. *J. Mol. Catal. A: Chem.* **2003**, *203*, 287. (d) Kishimoto, Y.; Eckerle, P.; Mitayake, T.; Kainosho, M.; Ono, A.; Ikariya, T.; Noyori, R. *J. Am. Chem. Soc.* **1999**, *121*, 12035. (e) Misumi, Y.; Masusa, T. *Macromolecules* **1998**, *31*, 7572. (f) Katayama, H.; Yamamura, K.; Miyaki, Y.; Ozawa, F. *Organometallics* **1997**, *16*, 4497. (g) Haupt, H.-J.; Schneidermeier, J. *J. Organomet. Chem.* **1996**, *506*, 41. (h) Kishimoto, Y.; Eckerle, P.; Mitayake, T.; Ikariya, T.; Noyori, R. *J. Am. Chem. Soc.* **1994**, *116*, 12131. (i) Alper, H.; Goldberg, Y. *J. Chem. Soc., Chem. Commun.* **1994**, 1209. (j) Yang, W.; Tabata, M.; Kobayashi, S.; Yokota, K. *Polym. J.* **1991**, *23*, 1135. (k) Furlani, A.; Napoletano, C.; Russo, M. V.; Camus, A.; Marsich, N. *J. Polym. Sci.* **1989**, *27*, 75. (l) Kern, R. J. *J. Polym. Sci.* **1969**, *7*, 621.

(15) (a) Schmidt, J. A. R.; Arnold, J. *Organometallics* **2002**, *21*, 3426. (b) Schmidt, J. A. R.; Arnold, J. *J. Am. Chem. Soc.* **2001**, *123*, 8424.

(16) Grant, G. J.; Lee, J. P.; Helm, M. D.; Van Der Veer, D. G.; Pennington, W. T.; Harris, J. L.; Mehne, L. F.; Klinger, D. W. *J. Organomet. Chem.* **2005**, *690*, 629.

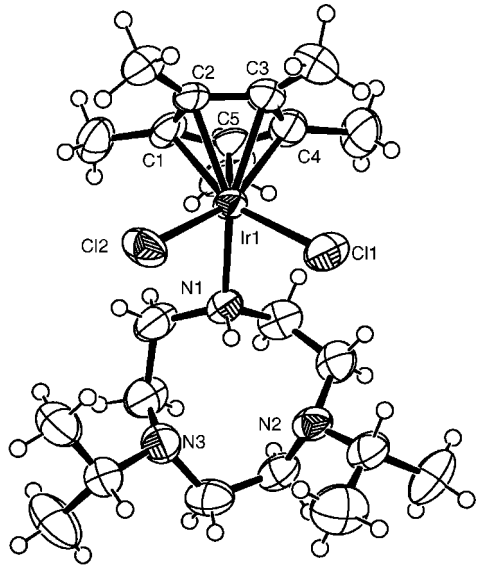

Figure 1. Molecular structure of **2**. Displacement ellipsoids are at the 50% probability level. Second molecule of asymmetric unit is omitted for clarity.

Table 2. Bond Lengths (Å) and Angles (deg) for 2

bond	length	bond	length
Ir(1)−N(1)	2.168(7)	Ir(1)−Cl(1)	2.415(2)
Ir(1)−Cl(2)	2.396(2)	Ir(1)−C(1)2.152(7)	2.152(4)
Ir(1)−C(2)	2.160(6)	Ir(1)−C(3)	2.173(7)
Ir(1)−C(4)	2.136(8)	Ir(1)−C(5)	2.163(8)
Ir(1)−Cp*$_{cent}$	1.776		
bonds	angle	bonds	angle
N(1)−Ir(1)−Cl(1)	85.04(19)	N(1)−Ir(1)−Cl(2)	85.11(19)
Cl(2)−Ir(1)−Cl(1)	88.70(9)		

the molecular structure (Figure 2) shows that all halide ligands have been scavenged and the macrocyclic ring is now coordinated in κ^3 fashion. The plane of symmetry bisecting the central Rh and the NH of the tacn ring is once again manifested in the $^{13}C\{^1H\}$ NMR spectra containing only three resonances corresponding to the macrocyclic ring. During the course of this work, the related complexes [(tacn)MCp*][PF_6]$_2$ were reported elsewhere.[16]

Synthesis of Rh(I) and Ir(I) Complexes. The results above led us to the investigation of the different binding modes of 1,4,7-triazacyclononane in forming Rh(I) and Ir(I) coordination complexes with the view to developing some structure−activity relationships in phenylacetylene polymerization. To this end, a series of Rh(I) and Ir(I) complexes **5**−**12** were prepared (**5** and **12** have been reported previously[2]), as shown in Scheme 2.

Treatment of [(COD)M(μ-Cl)$_2$] (M = Rh, Ir, COD = 1,5-cyclooctadiene) with 1,4-diisopropyl-1,4,7-triazacyclononane in THF yielded complexes **5** and **6**, which are analogous to complexes **1** and **2** in terms of the coordination geometry of the macrocycle, as elucidated by the X-ray crystal structure of **6**. Single crystals were obtained by vapor diffusion of diethyl ether into a saturated methylene chloride solution to yield triclinic crystals of the space group $P\bar{1}$. The molecular structure can be seen in Figure 3, and relevant bond lengths and angles can be found in Table 3. The coordination geometry about the central Ir is square planar in nature, consistent with 16-valence-electron complexes of M(I) (where M = Rh, Ir). The planes of symmetry bisecting the central Rh/Ir and the NH of the tacn ring observed in the crystal structures are once again manifested in the $^{13}C\{^1H\}$ NMR spectra of complexes **5** and **6**, containing only three resonances corresponding to the macrocyclic ring.

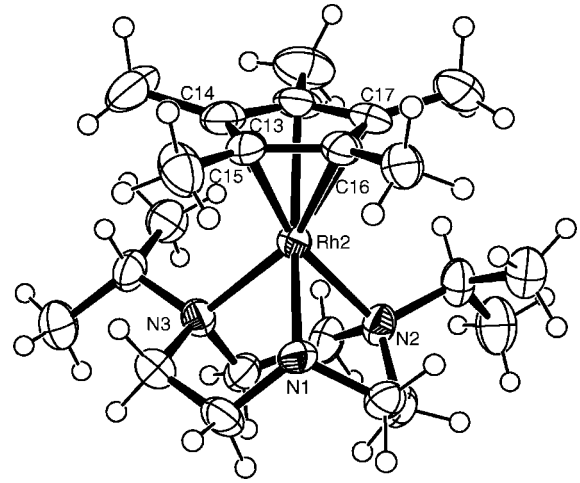

Figure 2. Molecular structure of **3**. Displacement ellipsoids are at the 50% probability level. Counterion, solvent of crystallization, and disordered second molecule of asymmetric unit are omitted for clarity.

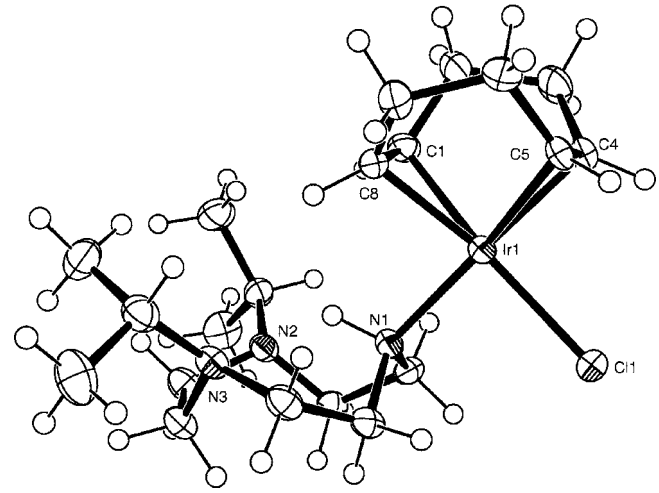

Figure 3. Molecular structure of **6**. Displacement ellipsoids are at the 50% probability level. Solvent of crystallization is omitted for clarity.

Table 3. Bond Lengths (Å) and Angles (deg) for 6

bond	length	bond	length
Ir(1)−N(1)	2.107(5)	Ir(1)−Cl(1)	2.3700(13)
Ir(1)−C(1)	2.117(5)	Ir(1)−C(4)	2.106(6)
Ir(1)−C(5)	2.125(6)	Ir(1)−C(8)	2.108(6)
bonds	angle	bonds	angle
Cl(1)−Ir(1)−N(1)	89.25(13)	Cl(1)−Ir(1)−C(4)	90.21(16)
Cl(1)−Ir(1)−C(5)	94.08(16)	N(1)−Ir(1)−C(1)	91.20(2)
N(1)−Ir(1)−C(8)	88.90(2)		

As demonstrated in the analogous conversion of complexes **1/2** to **3/4**, treatment of complexes **5** and **6** with various halide-abstracting agents cleanly yielded the air-stable complexes **7**−**9**. Complex **7** was synthesized by the reaction of **5** with silver trifluoromethanesulfonate, while complexes **8** and **9** were formed by Cl abstraction with $NaSbF_6$. The molecular structures of complexes **7**−**9** have been determined by X-ray crystallography; structural diagrams can be found in Figures 4–6, while relevant bond lengths and angles can be found in Tables 4–6. Single crystals of complex **7** were grown from a concentrated methanol solution stored at −18 °C. The coordination geometry about the central Rh in complex **7** (and in complexes **8** and **9**) is neither perfect square pyramidal or perfect trigonal bipyramidal

Scheme 2. Synthesis of Rh(I) and Ir(I) Complexes

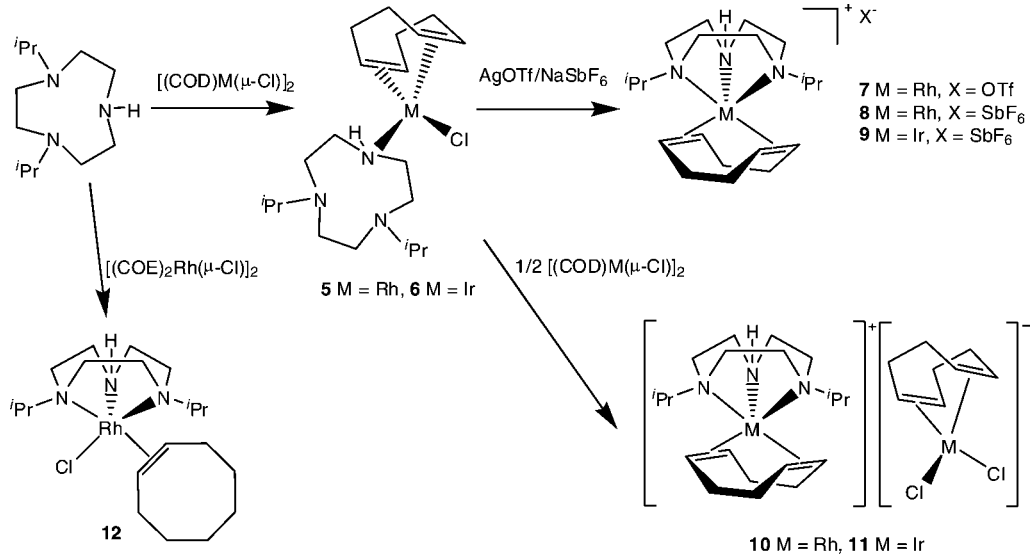

since the relevant N−M−N bite angles deviate significantly from the ideal 90° and 120° due to the geometric constraints of the facially coordinating macrocyclic ligand. The geometry can best be described as distorted trigonal bipyramidal. In all three structures, one M−N bond is considerably shorter than the other two; in all cases the unsubstituted nitrogen atom occupies an axial position *trans* to a double bond of the COD ligand and is ∼2.1 Å long. In contrast, the two "equatorial" nitrogen atoms are ca. 2.4 Å long. In all three structures the cyclooctadiene is in the expected "tub" conformation. In the structures of complexes **7** and **8** there are hydrogen bonds between the NH of the macrocyclic ring and the counteranion, to the oxygen of trifluoromethanesulfonate in complex **7** and the fluorine of

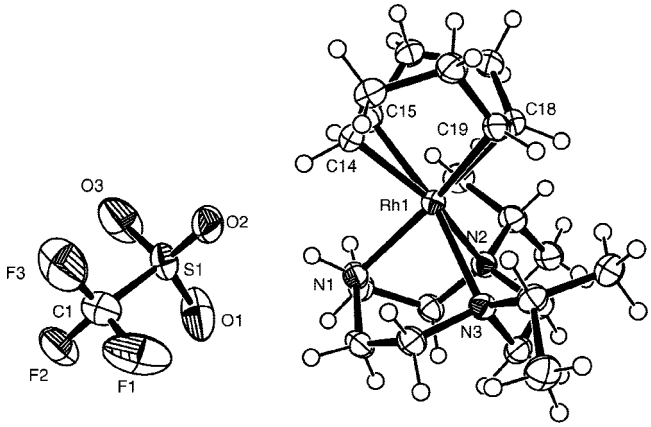

Figure 4. Molecular structure of **7**. Displacement ellipsoids are at the 50% probability level.

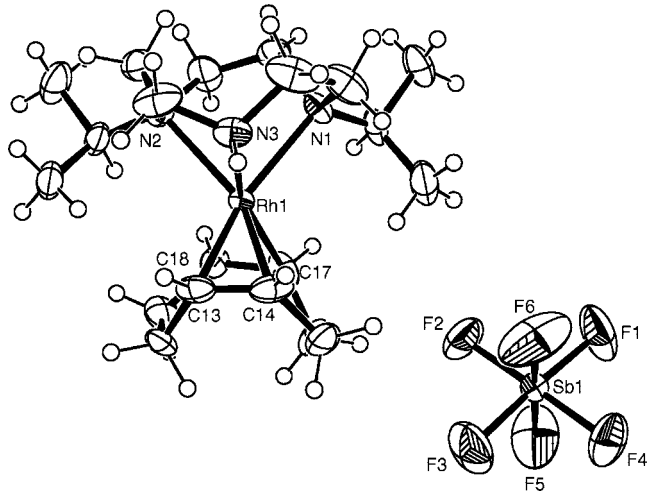

Figure 5. Molecular structure of **8**. Displacement ellipsoids are at the 50% probability level. Second and third molecules of the asymmetric unit are omitted for clarity.

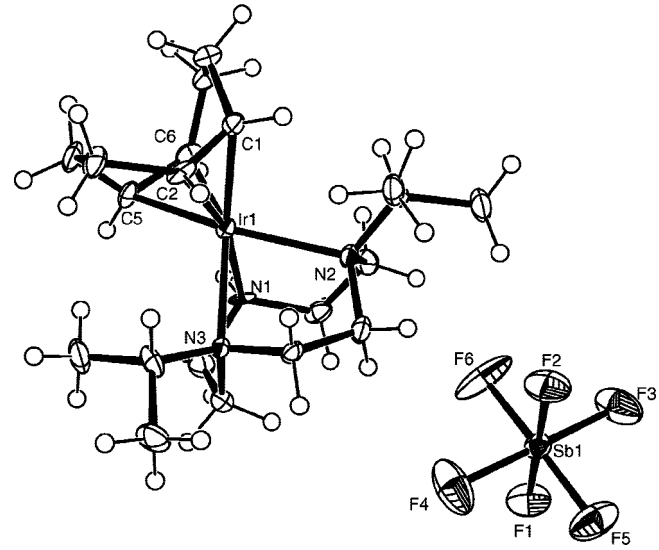

Figure 6. Molecular structure of **9**. Displacement ellipsoids are at the 50% probability level.

Table 4. Bond Lengths (Å) and Angles (deg) for 7

bond	length	bond	length
Rh(1)−N(1)	2.113(3)	Rh(1)−N(2)	2.456(3)
Rh(1)−N(3)	2.348(3)	Rh(1)−C(14)	2.091(3)
Rh(1)−C(15)	2.075(3)	Rh(1)−C(18)	2.141(3)
Rh(1)−C(19)	2.183(3)	N(1)−H(22)···O(2)	2.990
H(22)−O(2)	2.078		
bonds	angle	bonds	angle
N(1)−Rh(1)−N(2)	76.44(10)	N(1)−Rh(1)−N(3)	80.67(10)
N(3)−Rh(1)−N(2)	76.43(9)	C(19)−Rh(1)−N(3)	93.62(11)
C(18)−Rh(1)−N(2)	91.65(11)	N(1)−Rh(1)−C(14)	88.01(12)
N(1)−Rh(1)−C(15)	92.05(12)	C(14)−Rh(1)−C(19)	78.53(13)
C(15)−Rh(1)−C(18)	81.80(13)		

Table 5. Bond Lengths (Å) and Angles (deg) for 8

bond	length	bond	length
Rh(1)−N(1)	2.372(5)	Rh(1)−N(2)	2.413(6)
Rh(1)−N(3)	2.121(5)	Rh(1)−C(13)	2.070(7)
Rh(1)−C(14)	2.084(7)	Rh(1)−C(17)	2.170(7)
Rh(1)−C(18)	2.167(7)	N(6)−H(6)···F(11A)	2.902
H(6)···F(11A)	2.033		
bonds	angle	bonds	angle
N(1)−Rh(1)−N(2)	76.44(10)	N(1)−Rh(1)−N(3)	80.67(10)
N(2)−Rh(1)−N(3)	76.43(9)	N(1)−Rh(1)−C(17)	92.9(2)
N(2)−Rh(1)−C(18)	89.8(2)	N(3)−Rh(1)−C(13)	92.4(3)
N(3)−Rh(1)−C(14)	89.4(3)	C(13)−Rh(1)−C(18)	80.7(3)
C(14)−Rh(1)−C(17)	80.0(3)		

Table 6. Bond Lengths (Å) and Angles (deg) for 9

bond	length	bond	length
Ir(1)−N(1)	2.119(5)	Ir(1)−N(2)	2.316(5)
Ir(1)−N(3)	2.383(5)	Ir(1)−C(1)	2.157(6)
Ir(1)−C(2)	2.141(5)	Ir(1)−C(5)	2.072(6)
Ir(1)−C(6)	2.092(6)		
bonds	angle	bonds	angle
N(1)−Ir(1)−N(2)	80.2(2)	N(1)−Ir(1)−N(3)	76.9(2)
N(3)−Ir(1)−N(2)	77.10(17)	N(1)−Ir(1)−C(5)	91.5(3)
N(1)−Ir(1)−C(6)	87.6(2)	N(2)−Ir(1)−C(1)	93.1(2)
N(3)−Ir(1)−C(2)	91.8(2)	C(1)−Ir(1)−C(6)	78.4(3)
C(2)−Ir(1)−C(5)	82.0(3)		

Table 7. Bond Lengths (Å) and Angles (deg) for 10

bond	length	bond	length
Rh(1)−N(1)	2.113(5)	Rh(1)−N(2)	2.355(5)
Rh(1)−N(3)	2.423(5)	Rh(1)−C(1)	2.145(6)
Rh(1)−C(2)	2.194(6)	Rh(1)−C(5)	2.093(6)
Rh(1)−C(6)	2.083(6)	Rh(2)−Cl(1)	2.3827(15)
Rh(2)−Cl(2)	2.3778(15)	Rh(2)−C(21)	2.115(6)
Rh(2)−C(22)	2.118(7)	Rh(2)−C(25)	2.102(6)
Rh(2)−C(26)	2.099(7)	N(1)−H(29)···Cl(1)	3.267
Cl(1)···H(29)	2.381		
bonds	angle	bonds	angle
N(1)−Rh(1)−N(2)	80.38(17)	N(1)−Rh(1)−N(3)	76.92(17)
N(2)−Rh(1)−N(3)	77.01(16)	Cl(1)−Rh(2)−Cl(2)	91.13(5)

Table 8. Bond Lengths (Å) and Angles (deg) for 11

bond	length	bond	length
Ir(1)−N(1)	2.371(4)	Ir(1)−N(2)	2.112(4)
Ir(1)−N(3)	2.336(4)	Ir(1)−C(3)	2.133(5)
Ir(1)−C(4)	2.159(5)	Ir(1)−C(7)	2.076(5)
Ir(1)−C(8)	2.072(5)	Ir(2)−Cl(1)	2.3676(12)
Ir(2)−Cl(2)	2.3704(12)	Ir(2)−C(23)	2.088(5)
Ir(2)−C(24)	2.100(6)	Ir(2)−C(27)	2.087(5)
Ir(2)−C(28)	2.088(5)	N(2)−H(2)···Cl(2)	3.280
Cl(2)···H(2)	2.394		
bonds	angle	bonds	angle
N(1)−Ir(1)−N(2)	77.22(15)	N(1)−Ir(1)−N(3)	79.78(15)
N(2)−Ir(1)−N(3)	77.42(13)	Cl(1)−Ir(2)−Cl(2)	90.24(4)

hexafluoroantimonate in **8** with hydrogen bond lengths of 2.078 and 2.033 Å, respectively.

Synthesis of Rh(I) and Ir(I) Ion-Pair Complexes. When treated with a further half-equivalent of $[(COD)M(\mu\text{-}Cl)_2]$ (M = Rh, Ir, COD = 1,5-cyclooctadiene) in THF overnight, the novel, air-stable ion-pair complexes **10** and **11** were formed in high yield (Scheme 2). In these reactions the metal-COD dimer acts as a halide-abstracting reagent; the vacant coordination site on the metal complex is then occupied by the macrocyclic ligand. Attempted formation of mixed (Rh:Ir) metal complexes was unsuccessful. Though the $[M(COD)Cl_2]^-$ anion is known in Rh and Ir chemistry,[17] this is the first reported instance of this behavior with 1,4,7-triazacyclononane derivatives. The molecular structures of complexes **10** and **11** have been confirmed by X-ray crystallography and can be found in Figures 7 and 8. Relevant bond lengths and angles can be found in Tables 7 and 8. The coordination geometry about the cationic metal center in complexes **10** and **11** is distorted trigonal bipyramidal, with bond lengths and angles similar to complexes **7**−**9**. The geometry of the anionic portion of the structure can be described as near-perfect square planar, with Cl−M−Cl bite angles that deviate only slightly from the ideal angle of 90°. Hydrogen bonding is observed between the NH of the tacn moiety and a chlorine atom of the counterion. The hydrogen bond lengths have been determined as 2.381 and 2.396 Å in complexes **10** and **11**, respectively. The NMR spectra show a $^1J\{^{13}C\text{-}^{103}Rh\}$ of ca. 13−14 Hz between the carbon atoms of the cyclooctadiene moieties and Rh.

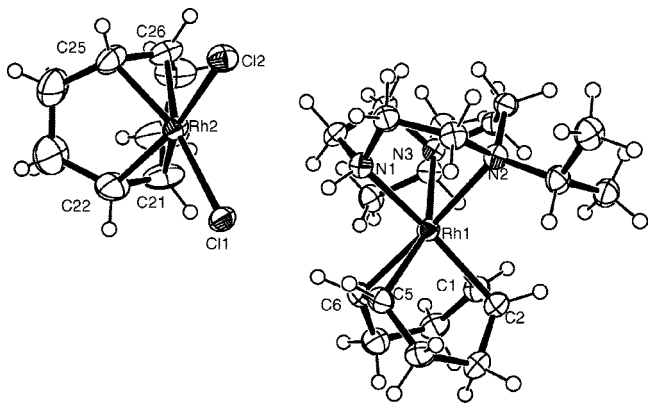

Figure 7. Molecular structure of **10**. Displacement ellipsoids are at the 50% probability level.

Initial Catalytic Screen. The complexes **5**−**12** were screened for catalytic activity in the polymerization of phenylacetylene compared to the $[M(COD)(\mu\text{-}Cl)]_2$ (M = Rh and Ir) dimers as well to each other. The initial catalyst screen data are displayed in Table 9.

The initial screening studies revealed that yields and molecular weights of the polymers are significantly greater than those obtained for $[M(COD)(\mu\text{-}Cl)]_2$ (M = Rh and Ir). The highest yields were obtained with the rhodium COD complexes. The average molecular weights were in the range of approximately 3000−9000 $gmol^{-1}$ for both metals and are greater than those obtained for $[M(COD)(\mu\text{-}Cl)]_2$ (M = Rh and Ir in most cases). The polydispersities revealed a broad range of molecular weights in the polymer samples. The lowest polydispersity values obtained were 2.1 and 2.2 for complex **8**. Generally, the polydispersity values were lower for the rhodium complexes. It was noted that some polymer yields increased with a higher temperature, whereas others decreased. The stereoregularity of the polymers shows that high percentages of the *cis*−*transoidal* isomer were obtained with the rhodium complexes **5** and **12** when compared to the control experiments using $[Rh(COD)(\mu\text{-}Cl)]_2$, where the opposite ratio was the case. It should be noted that in comparing **9** with **11** the counterion could have a bearing on the catalytic activity of **11**, although it is difficult to make the comparison between **7/8** and **10** because all three species are catalytically active.

Effect of Solvent. The reactions carried out in different solvents were performed under the same conditions as the initial screen, at a temperature of 40 °C. For the rhodium complex **5**, the average molecular weight approximately doubled in THF and toluene compared to using dichloromethane as the solvent, but to the detriment of the *cis*-content and polydispersity. Water had an adverse effect on the yield and polydispersity. For complex **8**, all three solvents increased yields, but gave poor polydispersity and *cis*-content of the polymers. In general for

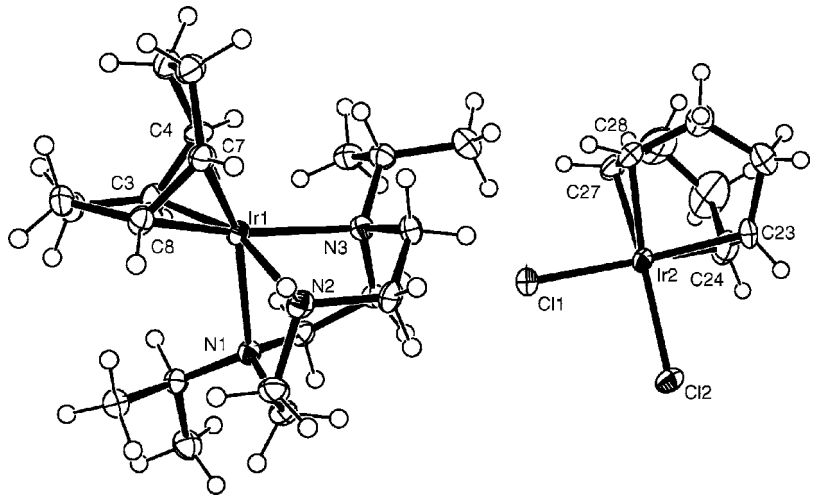

Figure 8. Molecular structure of **11**. Displacement ellipsoids are at the 50% probability level.

the iridium complex **6**, THF and toluene slightly increased the molecular weights compared to using dichloromethane as the solvent, but yields and polydispersities were approximately the same. Water had an adverse effect on the polymer properties, but all three solvents lowered the *cis*-content.

Effect of Added Base. The results in Table 10 also highlight the effect of adding a base to the reactions, as for some catalyst systems in the literature the addition of base improves the polydispersity of the polymers.[13] The actual mechanism is unknown, although it is thought that addition of base can neutralize acidic species that terminate the growing polymer chains. In these experiments, 10 equiv of either 4-dimethylaminopyridine (DMAP) or sodium methoxide was added to the dichloromethane solution prior to the addition of monomer. The experiments were performed at 40 °C. The addition of base increased the polydispersity values for the polymers obtained

Table 9. Initial Polymerization Screen

catalyst precursor	temperature (°C)	yield (%)	M_w (g mol^{-1})	M_n (g mol^{-1})	M_w/M_n	*cis*-content (%)
$[Rh(COD)Cl]_2$	21	4.0	2855	1375	2.1	14.1
5	22	>99	5060	1450	3.5	87.2
7	21	31.1	3130	1335	2.4	39.3
8	21	25.5	3485	1630	2.1	21.1
10	21	94.4	8620	2215	3.9	55.1
12	22	2.1	4860	1395	3.5	
$[Ir(COD)Cl]_2$	21	8.2	4570	1570	3.0	70.9
6	21	9.0	7475	1545	4.9	58.4
9	22	0				
11	21	6.1	4415	1565	2.8	51.2
$[Rh(COD)Cl]_2$	40	18.3	3035	1425	2.1	50.0
5	40	>99	5965	1540	3.9	87.2
7	40	81.2	5015	1740	2.9	40.0
8	40	44.5	3860	1740	2.2	30.1
10	40	84.2	5840	1555	3.8	22.8
12	40	5.80	4895	1165	4.3	73.7
$[Ir(COD)Cl]_2$	40	11.0	3935	1130	3.5	50.0
6	40	9.8	3240	1290	2.6	68.6
9	40	0				
11	40	13.2	3535	1115	3.2	55.8

Table 10. Results of Variation of Solvent and Base

catalyst ecursor	solvent	yield (%)	M_w (g mol^{-1})	M_n (g mol^{-1})	M_w/M_n	*cis*-content (%)
5	THF	>99	10 850	2285	4.8	30.6
5	toluene	>99	13 300	2700	5.0	70.6
5	water	68.2	12 750	1945	6.6	47.6
5 + DMAP	CH_2Cl_2	96.8	13 400	2135	6.3	75.0
5 + NaOMe	CH_2Cl_2	89.3	11 200	2210	5.1	35.3
8	THF	>99	7910	1915	4.1	
8	toluene	68.3	3995	1430	2.8	22.6
8	water	77.1	17 700	2405	7.4	30.8
8 + DMAP	CH_2Cl_2	69.7	6630	1605	4.2	70.3
8 + NaOMe	CH_2Cl_2	26.6	3625	1140	3.2	24.8
6	THF	9.0	4180	1880	2.3	38.5
6	toluene	9.3	5500	2090	2.7	43.9
6	water	3.1	2640	590	4.5	
6 + DMAP	CH_2Cl_2	0.8	2320	1105	2.2	
6 + NaOMe	CH_2Cl_2	3.2	4415	1560	2.9	10.0

Table 11. Variation of Reaction Time

catalyst	time (h)	yield (%)	M_w ($gmol^{-1}$)	M_n ($gmol^{-1}$)	M_w/M_n	*cis*-content (%)
8	3	4.4	2515	1030	2.4	44.3
8	6	13.3	2845	1130	2.5	37.3
8	12	6.9	3435	1255	2.8	12.6
	catalyst					
8	1/10	8.3	3135	1325	2.4	14.3
8	1/2	58.9	5980	1350	4.5	61.6
8	2	89.4	3640	1200	3.0	39.7

in the reactions with complexes **5** and **8**. For complex **6** the polydispersity was reduced to 2.2 from 2.6 by the addition of DMAP. Sodium methoxide did not improve any of the polymer properties obtained with all three complexes.

Effect of Reaction Time. Some reactions were carried out with varying reaction times. These were conducted at 40 °C in dichloromethane with complex **8**, which gave the best polymer polydispersities. The reactions were terminated after 3, 6, and 12 h. The results are displayed in Table 11. The *cis*-content was reduced as reaction time increased. In comparison to the reaction run for 24 h, the yield of polymer decreased for shorter runs from 30.1% to 4.4%. An increase in average molecular weight was observed between 3 and 12 h, from 2515 to 3435 g mol^{-1}. After 24 h, this was 3860 g mol^{-1}.

Effect of Catalyst Precursor Loading. Displayed in Table 11 are the results obtained when varying the concentration of catalyst precursor, using complex **8** only. The effect of increasing the catalyst precursor loading was to increase polymer yield from 8% to 90% and the *cis*-content from 14% to 40% with a concomitant increase in polydispersity. The molecular weights were similar to previous results, apart from the polymer isolated from the reaction in which the loading was halved. The molecular weight increased to ~6000 g mol^{-1}, compared to ~3000−4000 $gmol^{-1}$ for all others.[18]

Conclusions

The preparation of M(I) and M(III) (M = Rh, Ir) complexes containing 1,4-diisopropyl-1,4,7-triazacyclononane coordinated through one nitrogen atom was achieved; subsequent control of the coordination geometry was successful by a halide-abstracting reagent. The results of the catalytic studies show that the Rh(I) and Ir(I) complexes reported herein polymerize phenylacetylene more effectively than $[M(COD)(\mu\text{-Cl})]_2$ (M = Rh and Ir). Overall the complexes containing a κ^1-bound 1,4,7-triazacyclononane ligand gave higher yields and *cis*-content of polymer than the κ^3 derivatives.

Experimental Details

General Considerations. Unless otherwise stated, all manipulations involving the synthesis of novel compounds were conducted using standard Schlenk line techniques under an inert atmosphere of dry dinitrogen using a dual-manifold vacuum/dinitrogen line, or in a Braun Labmaster 100 glovebox. Dry dinitrogen was obtained by passing nitrogen gas through a double column of self-indicating diphosphorus pentoxide and activated 4 Å molecular sieves. All glassware, cannulas, and filter papers were stored in an oven at 150 °C overnight. Solvents were predried (where necessary) over the appropriate drying agent and then distilled under an atmosphere of dinitrogen: tetrahydrofuran from potassium; diethyl ether from sodium/benzophenone; petroleum ether (bp 40−60 °C), toluene, and pentane from sodium; methanol, methylene chloride, and acetonitrile from calcium hydride; acetone from potassium carbonate. All solvents were stored in glass ampules prior to use.

Deuterated solvents were purchased from GOSS Scientific Ltd., Apollo Scientific Ltd., and Sigma-Aldrich Chemical Co., degassed using three freeze−pump−thaw cycles, and stored over a potassium mirror or activated 4 Å molecular sieves, where appropriate. $RhCl_3 \cdot 3H_2O$ and $IrCl_3 \cdot 3H_2O$ were generously loaned by Johnson Matthey Plc. 1,4-Diisopropyl-1,4,7-triazacyclononane,[19] $[RhCp^*Cl(\mu\text{-Cl})]_2$,[20] $[Rh(COD)(\mu\text{-Cl})]_2$,[21] $[Rh(COE)_2(\mu\text{-Cl})]_2$,[21] $[IrCp^*Cl(\mu\text{-Cl})]_2$,[22] $[Ir(COD)(\mu\text{-Cl})]_2$,[23] **1**, **5**, and **12**[2] were prepared according to published procedures.

NMR spectra were obtained on either a Bruker ARX 250 spectrometer or a Bruker ARX 300 spectrometer. ^1H and $^{13}C\{^1H\}$ NMR spectra were referenced internally using residual protio-solvent resonances relative to tetramethylsilane (δ = 0 ppm). Routine NMR assignments were confirmed where necessary by $^1H-^1H$ (COSY) or $^1H-^{13}C$ (HMQC) correlation experiments. Elemental analyses were obtained by the University of Leeds Microanalytical Service, School of Chemistry, University of Leeds. GPC data were obtained by Dr. Steve Holding and Dr. Martin Forrest at RAPRA Technology Ltd., Shropshire, UK. Mass spectra were obtained by the University of Leeds Mass Spectrometry Service and the EPSRC National Mass Spectrometry Service, University of Swansea.

$[Ir(\eta^5\text{-}Cp^*)(\kappa^1\text{-}\{(^iPr)_2[9]aneN_3\})(Cl)_2]$ (2). To a Schlenk tube charged with a solution of $[IrCp^*Cl\text{-}(\mu\text{-Cl})]_2$ (40.4 mg, 0.051 mmol) in methylene chloride (10 mL) was added 1,4-(diisopropyl)-1,4,7-triazacyclononane (25.2 mg, 0.12 mmol) in methylene chloride (1 mL). The red-orange solution became yellow immediately and was left to stir for 2 h at room temperature. The solvent was removed *in vacuo*, and the orange-yellow oily residue was washed with cold pentane (2 × 3 mL) and dried *in vacuo* to yield an orange microcrystalline solid. Orange single crystals suitable for X-ray crystallography were grown by the diffusion of diethyl ether vapor into a concentrated methylene chloride solution stored at 5 °C. Yield: 30.6 mg (49%). ^1H NMR (300.1 MHz, $CDCl_3$, 300 K): 0.96 (d, 6H, $^3J_{HH}$ = 6.5 Hz, CH_3 of isopropyl), 1.01(d, 6H, $^3J_{HH}$ = 6.6 Hz, CH_3 of isopropyl), 1.63 (s, 15H, CH_3 of Cp*), 2.34 (m, 2H, N-CH_2 ring), 2.45 (m, 2H, N-CH_2 ring), 2.83−2.92 (m, 4H of N-CH_2 ring, 2H, C-*H* of isopropyl overlap), 3.15 (m, 2H, N-CH_2 ring), 3.51 (m, 2H, N-CH_2 ring), 5.14 (s, br, 1H, N-*H*). $^{13}C\{^1H\}$ NMR (75.5 MHz, $CDCl_3$, 300 K): 9.5 (*C*H_3 Cp*), 17.6, 19.9 (*C*H_3 of isopropyl), 51.1 (N-*C*H_2 ring), 53.2 (*C*-H of isopropyl), 54.1, 57.9 (N-*C*H_2 ring), 84.8 (C_q of Cp*). Anal. Calcd for $C_{22}H_{42}N_3Cl_2Ir$: C, 43.2; H, 6.9; N, 6.9. Found: C, 43.2; H, 6.9; N, 6.9. MS (ES): *m/z* 363.0 ($[M^+] - (^iPr)_2[9]aneN_3 - Cl$), 214.2 ($(^iPr)_2[9]aneN_3 + H$).

$[Rh(\eta^5\text{-}Cp^*)(\kappa^3\text{-}\{(^iPr)_2[9]aneN_3\})][BF_4]_2$ (3). To a Schlenk tube charged with a suspension of $[RhCp^*Cl\text{-}(\mu\text{-Cl})]_2$ (70.0 mg, 0.11

(17) (a) Martinez, A. P.; Garcia, M. P.; Lahoz, F. J.; Oro, L. A. *Inorg. Chim. Acta* **2003**, *347*, 86. (b) Field, L. D.; Messerle, B. A.; Rehr, M.; Soler, L. P.; Hambley, T. W. *Organometallics* **2003**, 22. (c) Merola, J. S.; Husebo, T. L.; Matthews, K. E.; Franks, M. A.; Pafford, R.; Chirik, P. *High Tech.* **1995**, *5*, 33. (d) Imhoff, P.; van Asselt, R.; Elsevier, C. J.; Zoutberg, M. C.; Stam, C. H. *Inorg. Chim. Acta* **1991**, *184*, 73. (e) Fernandez, M. J.; Del Val, J. J.; Oro, L. A.; Palacios, F.; Barluenga, J. *Polyhedron* **1987**, *6*, 1999.

(18) It should be noted that for some of the catalyst runs the polymer GPC traces contained a small fraction of high molecular weight material, which was thought to be of a different composition from the bulk of the sample. When manipulating the data, this fraction was not included in the calculation of the molecular weight average, as it would have skewed the data slightly. The average molecular weights of these fractions are in the range 79 000−146 000 g mol^{-1} with polydispersities of 1.1−2.0. As these were present in only a small amount (which could not be accurately determined), subsequent investigations could not be conducted. The only complexes that did not produce the higher molecular weight material were **5** and **10**.

(19) Halfen, J. A.; Tolman, W. B. *Inorg. Synth.* **1998**, *32*, 75.

(20) White, C.; Yates, A.; Maitlis, P. M. *Inorg. Synth.* **1992**, *29*, 229.

(21) Giordano, G.; Crabtree, R. H. *Inorg. Synth.* **1979**, *19*, 218.

(22) Ball, R. G.; Graham, W. A. G.; Heinekey, D. M.; Hoyano, J. K.; McMaster, A. D.; Mattson, B. M.; Michel, S. T. *Inorg. Chem.* **1990**, *29*, 2023.

(23) Renate, F.; Sonja, K.; Richard, W. *Eur. Pat. Appl. EP1116724 A2*, 2001.

mmol) and sodium tetrafluoroborate (107.2 mg, 0.98 mmol) in THF (20 mL) was added 1,4-(diisopropyl)-1,4,7-triazacyclononane (48.0 mg, 0.225 mmol) in THF (5 mL). The red suspension became red-orange after stirring overnight at room temperature. The THF was removed *in vacuo* and the oily red residue extracted with methylene chloride (15 mL) and filtered. The filtrate was concentrated to ca. 5 mL and petroleum ether (20 mL) added. The product was isolated as a red microcrystalline solid by filtration, washed with petroleum ether (3 × 10 mL), and dried *in vacuo*. Red single crystals suitable for X-ray crystallography were grown by the slow diffusion of petroleum ether vapor into a concentrated methylene chloride solution. Yield: 55.4 mg (78%). ^{1}H NMR (300.13 MHz, $CDCl_3$, 300 K): 1.10 (d, 12H, $^3J_{HH}$ = 6.6 Hz, C*H*$_3$ of isopropyl), 1.71 (s, 15H, C*H*$_3$ of Cp*), 2.56 (s, 4H, N-C*H*$_2$ ring), 2.78 (t, 4H, N-C*H*$_2$ ring), 2.95 (sept, 2H, $^3J_{HH}$ = 6.6 Hz, C-*H* of isopropyl), 3.14 (m, br, 4H, N-C*H*$_2$ ring). ^{13}C{^{1}H} NMR (62.90 MHz, $CDCl_3$, 300 K): 9.2 (*C*H$_3$ Cp*), 18.7 (*C*H$_3$ of isopropyl), 43.8, 44.5, 46.3 (N-*C*H$_2$ ring), 52.63 (*C*-H of isopropyl), 95.1 (C_q of Cp*). Anal. Calcd for $C_{22}H_{42}N_3B_2F_8Rh.(C_7H_{16})_{0.2}$: C, 43.6; H, 7.1; N, 6.5. Found: C, 44.0; H 7.3; N, 7.1. MS (ES): *m*/*z* 538.3 ([M$^+$] − BF_4), 450.3 ([M$^+$] − H − 2BF_4), 214.2 ((^{i}Pr)$_2$[9]aneN$_3$ + H).

[Ir(η^5-Cp*)(κ^3-{(^{i}Pr)$_2$[9]aneN$_3$})][SbF$_6$]$_2$ (4). To a Schlenk tube charged with a solution of [IrCp*Cl-(μ-Cl)]$_2$ (26.8 mg, 0.034 mmol) in methylene chloride (10 mL) was added 1,4-(diisopropyl)-1,4,7-triazacyclononane (17.7 g, 0.083 mmol) in acetone (1 mL). The red-orange solution became yellow immediately. A solution of sodium hexafluoroantimonate (35.0 mg, 0.135 mmol) in acetone (2 mL) was added, resulting in the formation of a fine precipitate, after stirring at room temperature for 18 h. The solvent was removed *in vacuo* and the beige residue washed with methylene chloride (2 × 10 mL). Extraction with acetone (10 mL), followed by removal of the solvent *in vacuo*, yielded the title compound as a yellow microcrystalline solid, which was washed with petroleum ether (3 mL). Yield: 6.8 mg (10%). ^{1}H NMR (300.13 MHz, $(CD_3)_2CO$, 300 K): 1.46 (d, 6H, $^3J_{HH}$ = 6.3 Hz, CH_3 of isopropyl), 1.58 (d, 6H, $^3J_{HH}$ = 6.4 Hz, CH_3 of isopropyl), 1.77 (15H, CH_3 of Cp*), 3.18 (m, 2H, N-CH_2 ring), 3.31−3.68 (m, 8H, N-CH_2 ring), 3.65 (m, 2H, N-CH_2 ring), 4.02 (sept, $^3J_{HH}$ = 6.4 Hz, 2H, C-H of isopropyl), 7.58 (br, 1H, N-H). ^{13}C{^{1}H} NMR (75.47 MHz, $(CD_3)_2CO$, 300 K): 10.0 (CH_3 Cp*), 18.9, 22.8 (CH_3 of isopropyl), 56.6, 58.5, 61.2 (N-CH_2 ring), 66.3 (C-H of isopropyl), 92.5 (C_q of Cp*). Anal. Calcd for $C_{22}H_{42}N_3F_{12}IrSb_2\cdot(CH_2Cl_2)_{0.5}$: C, 25.6; H, 4.1; N, 4.0. Found: C, 25.5; H, 4.2; N, 4.0. MS (ES): *m*/*z* 775.7 ([M$^+$] − H − SbF_6), 540.0 ([M$^+$] − H − SbF_6), 214.1 ((^{i}Pr)$_2$[9]aneN$_3$ + H).

[Ir(η^4-COD)(κ^1-{(^{i}Pr)$_2$[9]aneN$_3$})Cl] (6). To a Schlenk tube charged with a solution of [Ir(COD)(μ-Cl)]$_2$ (112.7 mg, 0.17 mmol) in THF (10 mL) was added 1,4-(diisopropyl)-1,4,7-triazacyclononane (73.0 g, 0.34 mmol) in THF (1 mL). After stirring at room temperature for 6 h, the solution turned yellow. The solvent was removed *in vacuo*, and the oily yellow residue was washed with petroleum ether (3 × 10 mL). The remaining yellow microcrystalline solid was dried *in vacuo*. Yellow single crystals suitable for X-ray crystallography were grown by diffusion of diethyl ether vapor into a concentrated methylene chloride solution stored at 5 °C. Yield: 85.0 mg (46%). ^{1}H NMR (300.13 MHz, $C_6D_5(CD_3)$, 300 K): 0.70 (d, $^3J_{HH}$ = 6.5 Hz, 6H, C*H*$_3$ of isopropyl), 0.78 (d, $^3J_{HH}$ = 6.7 Hz, 6H, C*H*$_3$ of isopropyl), 1.33−1.45 (m, 4H, C*H*$_2$ of COD), 1.65 (m, 2H, N-C*H*$_2$ ring), 1.93 (m, 2H, N-C*H*$_2$ ring), 2.13 (m, 4H, C*H*$_2$ of COD, 2H, N-C*H*$_2$ ring), 2.31 (m, 2H, N-C*H*$_2$ ring), 2.48 (sept, $^3J_{HH}$ = 6.6 Hz, 2H, C-*H* of isopropyl), 3.09 (m, 2H, N-C*H*$_2$ ring), 3.17 (m, 2H, C*H* of COD), 4.56 (m, 2H, C*H* of COD), 6.06 (s, br, 1H, N-*H*). ^{13}C{^{1}H} NMR (75.47 MHz, $C_6D_5(CD_3)$, 300 K): 15.38, 18.54 (*C*H$_3$ of isopropyl), 30.28, 31.48 (*C*H$_2$ of COD), 44.44, 44.99, 47.42 (N-*C*H$_2$ ring), 51.99 (*C*-H of isopropyl), 52.92, 65.32 (*C*H of COD). Anal. Calcd for $C_{20}H_{39}N_3ClIr$: C, 43.7; H, 7.2; N, 7.7. Found: C, 43.9; H, 7.1; N, 7.6. MS (ES): *m*/*z* 514.2 ([M$^+$] + H − Cl), 214.2 ((^{i}Pr)$_2$[9]aneN$_3$ + H).

[Rh(η^4-COD)(κ^3-{(^{i}Pr)$_2$[9]aneN$_3$})][OTf] (7). To a Schlenk tube charged with a solution of **5** (74.3 mg, 0.164 mmol) in THF (2 mL) was added silver trifluoromethanesulfonate (43.2 mg, 0.168 mmol) in THF (1 mL). The yellow solution was allowed to stir for 1 h at room temperature in the dark. A pale precipitate was seen to form immediately. The yellow suspension was filtered, the remaining white solid was washed with methylene chloride (10 mL), and the filtrates were combined. The solvent was removed *in vacuo* from the filtrates, and the yellow residue was washed with diethyl ether (2 × 5 mL) and dried *in vacuo* to yield a yellow microcrystalline solid. Yellow single crystals suitable for X-ray crystallography were grown from a concentrated methanol solution stored at −18 °C. Yield: 26.8 mg (29%). ^{1}H NMR (300.13 MHz, $(CD_3)_2CO$, 300 K): 1.20 (d, $^3J_{HH}$ = 6.4 Hz, 6H, C*H*$_3$ of isopropyl), 1.67 (m, 10H, overlap, 6H C*H*$_3$ of isopropyl, 4H C*H*$_2$ of COD), 2.41 (m, 4H, C*H*$_2$ of COD), 2.70−2.90 (m, overlap with solvent, N-C*H*$_2$ ring), 3.18 (m, 2H, N-C*H*$_2$ ring), 3.31 (m, 2H, N-C*H*$_2$ ring), 3.63 (s, br, 4H, C*H* of COD), 3.95 (sept, $^3J_{HH}$ = 6.4 Hz, 2H, C-*H* of isopropyl), 4.55 (s, br, 1H, N-*H*). ^{13}C{^{1}H} NMR (75.48 MHz, $(CD_3)_2CO$, 300 K): 17.3, 22.5 (*C*H$_3$ of isopropyl), 31.9 (*C*H$_2$ of COD), 50.0, 54.0 (br, N-*C*H$_2$ ring), 59.2 (*C*-H of isopropyl), 74.3 (m, br, *C*H of COD), 124.5 (*C* of CF_3SO_3). Anal. Calcd for $C_{21}H_{39}N_3F_3O_3RhS$: C, 44.0; H, 6.9; N, 7.3. Found: C, 43.7; H, 7.0; N, 7.1. MS (ES): *m*/*z* 423.9 ([M$^+$] − [O_3SCF_3]), 213.9 ((^{i}Pr)$_2$-[9]aneN$_3$ + H).

[Rh(η^4-COD)(κ^3-{(^{i}Pr)$_2$[9]aneN$_3$})][SbF$_6$] (8). To a Schlenk tube charged with a solution of **5** (26.1 mg, 0.057 mmol) in THF (1 mL) was added excess sodium hexafluoroantimonate (59.3 mg, 0.23 mmol) in acetone (1 mL). After stirring at room temperature for 18 h, a pale precipitate was seen to form. The yellow suspension was filtered, the remaining white solid was washed with THF (10 mL), and the filtrates were combined. The solvent was removed *in vacuo* and the resulting yellow residue washed with petroleum ether (5 mL) and dried to yield a yellow solid. This was recrystallized from a concentrated acetone solution stored at −18 °C. Yellow single crystals suitable for X-ray crystallography were grown by the diffusion of diethyl ether vapors into a concentrated acetone solution stored at 5 °C. Yield: 30.7 mg (82%). ^{1}H NMR (300.13 MHz, $(CD_3)_2CO$, 300 K): 1.17 (d, $^3J_{HH}$ = 6.3 Hz, 6H, C*H*$_3$ of isopropyl), 1.68 (m, 10H, overlap, d, $^3J_{HH}$ = 6.6 Hz, 6H, C*H*$_3$ of isopropyl, 4H C*H*$_2$ of COD), 2.41 (m, br, 4H, C*H*$_2$ of COD), 2.74−2.97 (m, overlap with solvent, N-C*H*$_2$ ring), 3.16 (m, 2H, N-C*H*$_2$ ring), 3.32 (m, 2H, N-C*H*$_2$ ring), 3.61 (br, 4H, C*H* of COD), 3.91 (sept, $^3J_{HH}$ = 6.4 Hz, 2H, C-*H* of isopropyl), 4.38 (br, 1H, N-*H*). ^{13}C{^{1}H} NMR (75.48 MHz, $(CD_3)_2CO$, 300 K): 17.3, 22.5 (*C*H$_3$ of isopropyl), 31.8 (*C*H$_2$ of COD), 50.1, 54.1 (br, N-*C*H$_2$ ring), 59.3 (*C*H of isopropyl), 74.4 (br, *C*H of COD). Anal. Calcd for $C_{20}H_{39}N_3F_6RhSb$: C, 36.4; H, 6.0; N, 6.4. Found: C, 35.5; H, 6.1; N, 6.3. MS (ES): *m*/*z* 423.9 ([M$^+$] − [SbF_6]), 213.9 ((^{i}Pr)$_2$-[9]aneN$_3$ + H).

[Ir(η^4-COD)(κ^3-{(^{i}Pr)$_2$[9]aneN$_3$})][SbF$_6$] (9). To a Schlenk tube charged with a solution of [Ir(COD)(μ-Cl)]$_2$ (43.3 mg, 0.065 mmol) in THF (10 mL) was added 1,4-(diisopropyl)-1,4,7-triazacyclononane (28.8 mg, 0.135 mmol) in THF (1 mL). After stirring at room temperature for 4 h, sodium hexafluoroantimonate (69.7 mg, 0.269 mmol) in acetone (2 mL) was added to the yellow solution. After stirring at room temperature for a further 18 h, a fine precipitate was observed. The solvent was removed *in vacuo* and the residue extracted with methylene chloride (2 × 10 mL) and filtered. The solvent was removed *in vacuo* and the oily yellow residue washed with petroleum ether (2 × 10 mL) to yield a pale yellow microcrystalline solid, which was dried *in vacuo*. Yellow single crystals suitable for X-ray crystallography were grown from a concentrated acetone solution stored at 5 °C. Yield: 62.0 mg (64%). ^{1}H NMR (300.13 MHz, $(CD_3)_2CO$, 300 K): 1.22 (d, 6H, $^3J_{HH}$ = 6.3 Hz, C*H*$_3$ of isopropyl), 1.32 (m, 4H, C*H*$_2$ of COD), 1.62 (d, 6H, $^3J_{HH}$ = 6.5 Hz, C*H*$_3$ of isopropyl), 2.22 (m, br, 4H,

CH_2 of COD), 2.80 (m, 2H, N-CH_2 ring), 2.92−3.35 (m, 10H, N-CH_2 ring), 3.20 (s, br, 4H, C*H* of COD), 3.95 (sept, 2H, $^3J_{HH}$ = 6.4 Hz, C-*H* of isopropyl), 5.27 (s, br, 1H, N-*H*). $^{13}C\{^1H\}$ NMR (75.47 MHz, $(CD_3)_2CO$, 300 K): 17.0, 23.0 (*C*H_3 of isopropyl), 32.9 (*C*H_2 of COD), 51.9, 56.5, 56.9 (N-*C*H_2 ring), 60.5 (*C*-H of isopropyl), COD *C*-H not observed. Anal. Calcd for $C_{20}H_{39}N_3F_6IrSb$: C, 32.1; H, 5.2; N, 5.6. Found: C, 32.2; H, 5.3; N, 5.7. MS (ES): *m*/*z* 512.1 ([M^+] − H − SbF_6), 214.2((^{i}Pr)$_2$[9]aneN$_3$ + H).

[Rh(η^4-COD)(κ^3-{(^{i}Pr)$_2$[9]aneN$_3$})][Rh(COD)Cl$_2$] (10). To a Schlenk tube charged with a solution of **5** (42.7 mg, 0.093 mmol) in THF (2 mL) was added [Rh(COD(μ-Cl)]$_2$ (23.0 mg, 0.047 mmol) in THF (2 mL). After stirring at room temperature for 18 h, the solvent was removed *in vacuo* from the yellow solution. The resulting pale yellow residue was washed with petroleum ether (3 × 10 mL) and dried *in vacuo*, to yield a pale yellow microcrystalline solid. Yellow single crystals suitable for X-ray crystallography were grown from a concentrated toluene solution stored at 5 °C. Yield: 29.6 mg (89%). ^1H NMR (300.13 MHz, $C_6D_5(CD_3)$, 300 K): 0.72 (d, $^3J_{HH}$ = 6.5 Hz, 6H, C*H*$_3$ of isopropyl), 0.72 (d, $^3J_{HH}$ = 6.7 Hz, 6H, C*H*$_3$ of isopropyl), 1.30 (m, br, 4H, CH_2 of COD), 1.58 (m, br, 4H, CH_2 of COD), 1.69 (m, 2H, N-CH_2 ring), 1.92 (m, overlap with solvent, N-CH_2 ring), 2.12−2.33 (m, overlap, 8H, 4H CH_2 of COD, 4H N-CH_2 ring), 2.52 (sept, $^3J_{HH}$ = 6.6 Hz, 2H, C-*H* of isopropyl), 3.15 (m, 2H, N-CH_2 ring), 3.46 (s, br, 2H, C*H* of COD), 4.20 (s, br, 4H, C*H* of COD), 4.80 (s, br, 2H, C*H* of COD), 4.90 (s, br, 1H, N-*H*). $^{13}C\{^1H\}$ NMR (75.48 MHz, $C_6D_5(CD_3)$, 300 K): 15.7, 19.1 (*C*H_3 of isopropyl), 29.4, 29.6, 30.6 (*C*H_2 of COD), 44.8, 45.1, 47.0 (N-*C*H_2 ring), 52.0 (*C*-H of isopropyl), 70.8 (d, $^1J_{RhC}$ = 14.3 Hz, *C*H of COD), 77.0 (d, $^1J_{RhC}$ = 13.4 Hz, *C*H of COD), 81.3 (d, $^1J_{RhC}$ = 11.3 Hz, *C*H of COD). Anal. Calcd for $C_{28}H_{51}N_3Cl_2Rh_2$: C, 47.6; H, 7.3; N, 6.0. Found: C, 47.0; H, 7.5; N, 5.6. MS (ES): *m*/*z* 424.3 ([M^+] − H − [(COD)Cl_2Rh]), 214.2 ((^{i}Pr)$_2$[9]aneN$_3$ + H).

[Ir(η^4-COD)(κ^3-{(^{i}Pr)$_2$[9]aneN$_3$})][Ir(COD)Cl$_2$] (11). To a Schlenk tube charged with a solution of **6** (21.0 mg, 0.0382 mmol) in THF (3 mL) was added [Ir(COD(μ-Cl)]$_2$ (13.3 mg, 0.0198 mmol) in THF (2 mL). After stirring at room temperature for 24 h, the resulting yellow solution was concentrated to ca. 1 mL *in vacuo* and petroleum ether (20 mL) was added. The product was isolated as a pale yellow microcrystalline solid by filtration, washing with petroleum ether (2 × 20 mL), and drying *in vacuo*. Yellow single crystals suitable for X-ray crystallography were grown from a concentrated acetonitrile solution stored at 5 °C. Yield: 30.2 mg (89%). ^1H NMR (300.13 MHz, $CDCl_3$, 300 K): 1.17 (d, $^3J_{HH}$ = 6.4 Hz, 6H, C*H*$_3$ of isopropyl), 1.31 (m, 6H, overlap, CH_2 of COD), 1.55 (d, $^3J_{HH}$ = 6.5 Hz, 6H, C*H*$_3$ of isopropyl), 2.13 (m, br, 6H, CH_2 of COD), 2.61−2.76 (m, 4H, N-CH_2 ring), 2.94 (m, 2H, N-CH_2 ring), 3.12 (m, 4H, N-CH_2 ring), 3.28 (s, br, 4H, C*H* of COD), 3.46 (m, 2H, N-CH_2 ring), 3.78 (sept, $^3J_{HH}$ = 6.4 Hz, 2H, C-*H* of isopropyl), 3.90 (s, br, 2H, C*H* of COD), 6.15 (s, br, 1H, N-*H*). $^{13}C\{^1H\}$ NMR (75.48 MHz, $CDCl_3$, 300 K): 17.3, 22.5 (*C*H_3 of isopropyl), 32.2, 32.4 (*C*H_2 of COD), 51.3, 55.3, 55.6 (N-*C*H_2 ring), 59.4 (*C*-H of isopropyl), 60.2 (s, *C*H of COD). Anal. Calcd for $C_{28}H_{51}N_3Cl_2Ir_2$: C, 38.0; H, 5.8; N, 4.8. Found: C, 37.8; H, 5.8; N, 4.4. MS (ES): *m*/*z* 514.1 ([M^+] − H − [(COD)Cl_2Ir]), 211.1 ((^{i}Pr)$_2$[9]aneN$_3$ − 2H).

Polymerization Catalysis. The reactions were carried out in dry methylene chloride (5 mL) under an atmosphere of dry dinitrogen. The catalyst to phenylacetylene loadings were all ∼0.04:4 mmol (ratio 1:100), and the reactions were allowed to stir at either room temperature or 40 °C for 24 h. The resulting viscous red solutions were poured into acidified methanol, precipitating the polymeric products as orange-brown solids, which were filtered and dried in air. The polymers were characterized by ^1H NMR and $^{13}C\{^1H\}$ NMR spectroscopy in $CDCl_3$. Molecular weight determinations were carried out by GPC calibrated against monodisperse polystyrene standards. Control experiments were also undertaken using the same reaction conditions as the catalyst screen, with [M(COD)(μ-Cl)]$_2$ (M = Rh and Ir).

X-ray Crystallography. X-ray diffraction data for **2**, **3**, and **6**−**11** were collected on a Nonius KappaCCD area detector diffractometer using graphite-monochromated Mo Kα radiation (λ = 0.71073 Å). A typical procedure is given. A suitable single crystal was selected and immersed in an inert oil. It was mounted on a glass capillary and attached to the goniometer head of a Nonius KappaCCD area detector diffractometer cooled to 150 K by an Oxford Cryosystems low-temperature device.[24] Preliminary unit cell data were obtained by ten 20 s exposures, before full data acquisition. The images were processed using the DENZO and SCALEPACK[25] programs. Structure solution by direct methods was achieved through the use of one of the SHELXS86,[26] SIR92,[27] and SIR97[28] programs, and the structural model refined by full-matrix least-squares on F^2 using SHELXL97.[29] Molecular graphics were plotted using POV-RAY[30] via the XSeed[31] program or ORTEP-3.[32] Unless stated to the contrary, hydrogen atoms were placed using idealized geometric positions (with free rotation for methyl groups), allowed to move in a "riding model" along with the atoms to which they were attached, and refined isotropically; *U*(H) was set at 1.2 × (1.5 × for methyl groups) U_{eq} for the parent atom.

Acknowledgment. We thank the EPSRC for financial support (Ph.D. studentship to C.T.) and Johnson Matthey PLC for generous loans of $RhCl_3 \cdot 3H_2O$ and $IrCl_3 \cdot 3H_2O$. We acknowledge the assistance of Dr. Michaele J. Hardie and Mr. Colin A. Kilner for assistance with X-ray crystallography, and the EPSRC National Mass Spectrometry Service, University of Swansea, UK.

Supporting Information Available: Crystallographic information files for the structural determinations of **2**, **3**, and **6**−**11**. These can be found free of charge via the Internet at http://pubs.acs.org.

OM800180A

(24) Cosier, J.; Glazer, A. M. *J. Appl. Crystallogr.* **1986**, *19*, 105.
(25) Otwinowski, Z.; Minor, W. *DENZO and SCALEPACK programs*; Yale University: New Haven, CT, 1995.
(26) Sheldrick, G. M. *SHELXS86, Program for Crystal Structure Solution*; University of Gottingen, 1986.
(27) Altomare, A.; Burla, M. C.; Camalli, M.; Cascarno, M.; Giacavazzo, C.; Guagliardi, A.; Polidori, G. *J. Appl. Crystallogr.* **1993**, *26*, 343.
(28) Altomare, A.; Burla, M. C.; Camalli, M.; Cascarno, M.; Giacavazzo, C.; Guagliardi, A.; Moliterni, A. G. G.; Polidori, G.; Spagna, R. *J. Appl. Crystallogr.* **1999**, 32.
(29) Sheldrick, G. M. *SHELXL97, Program for Crystal Structure Refinement*; University of Gottingen, 1997.
(30) *POVray*: *Persistence of Vision Raytracer, 3.6*; Persistence of Vision Pty. Ltd., 2004.
(31) Barbour, L. J. *J. Supramol. Chem.* **2001**, *1*, 189.
(32) Farrugia, L. J. *J. Appl. Crystallogr.* **1997**, *30*, 565.